09

Study of histological sections of muscle tissues using X-ray fluorescence and Raman spectromicroscopy

© I.A. Artyukov,[1] G.P. Arutyunov,[2] D.O. Dragunov,[2] N.N. Melnik,[1] D.H.A. Paneke,[1] E.V. Perevedentseva,[1] A.V. Sokolova,[2] V.V. Sokolova[1]

[1] P.N. Lebedev Physical Institute of the Russian Academy of Sciences,
119991 Moscow, Russia
[2] N.I. Pirogov Russian National Research Medical University,
117997 Moscow, Russia
e-mail: iart@lebedev.ru

Received April 7, 2023
Revised April 7, 2023
Accepted April 7, 2023

The paper presents the results of a study of the chemical composition of myocardial tissues and striated muscles at the cellular level using a combination of X-ray fluorescence microscopy and Raman microspectrosopy. The distribution of inorganic materials (Na, Si, Ca, etc.) was measured with the help of X-ray fluorescence imaging and microanalysis workstations at ELETTRA synchrotron (Italy). Methods of infrared Raman spectromicroscopy were applied for the identification of organic compounds (lipids, amides, and polysaccharides). All experiments were carried out with unstained paraffin-embedded histological sections. The research was related to the study of sodium deposits in muscle tissues.

Keywords: X-ray microscopy, Raman spectroscopy, histological sections, chemical fixation, sodium deposits.

DOI: 10.61011/TP.2023.07.56633.75-23

Introduction

As is known, there is a direct relation between an increase in daily salt intake and an increase in the number of cardiovascular diseases, including fatal ones (see, for example, [1]). The concept of the deposition of sodium in the skin and muscle tissue was first formulated in experiments in the 70s of the last century. Later in his studies, the German researcher J. Titze suggested that osmotically neutral sodium may exist in the body, which accumulates on negatively charged glycosaminoglycans (GAGs) in the interstitial space of muscle tissue, including the myocardium [2].

The excessive sodium content in interstitial in rat myocardial tissues spaces caused by excessive salt intake [3] was revealed in our previous work using X-ray microscopy methods. The purpose of the present work is to study the possibilities of a comprehensive study by X-ray and infrared spectroscopy of the chemical composition of the tissues of the striated muscles and myocardium of rats using a series of unstained histological sections prepared according to standard technology with chemical fixation in paraffin. X-ray fluorescence microscopy is highly sensitive to the presence of traces of chemical elements, while infrared Raman spectroscopy is an effective tool for the identification and localization of organic compounds, which should ultimately confirm the current hypothesis about the presence of deposits of non-osmotic sodium associated with glycosoaminoglycans in the interstitum [2].

X-ray fluorescence microscopy based on synchrotron radiation is successfully used for chemical analysis of various biological objects with nanometer spatial resolution, which allows visualizing a map of the distribution of chemical elements at the cellular and even subcellular level and revealing their pathology [4–6]. It should be noted that thin polymer films and membranes needs to be used as substrates in the soft X-ray radiation range of characteristic K-lines of light chemical elements (photon energy up to 1 keV) and samples should be prepared for use in ultrahigh vacuum conditions. Thin ($3-4\,\mu$m) unstained and dried histological sections prepared according to standard medical techniques satisfy this requirement. On the other hand, standard chemical fixation using formalin and treatment and paraffinization procedures significantly complicates the search for traces of washed-out light elements and does not allow the use of quantitative methods for microanalysis of prepared samples. Therefore, in this work, a comparative methodology and parametric analysis were developed and used to detect differences and features of the chemical composition of tissues of different groups of laboratory animals.

In addition to X-ray microscopy, the same histological unstained sections were examined by Raman spectroscopy with excitation in the infrared range. As is known, this spectroscopic analysis provides the key to determining the molecular structure of substances without the use of any specific chemical labeling and fluorescent dyes [7]. It should be noted that recently there has been a noticeable increase in the use of the Raman method in biological studies [8].

As a rule, significant regions of the Raman spectrum observed in biological samples fall within the range of wavenumbers $400-2000\,\mathrm{cm}^{-1}$ associated with vibra-

tions in protein bonds ($1500-1700\,cm^{-1}$), carbohydrates ($470-1200\,cm^{-1}$), DNA phosphate groups (980, 1080 and $1240\,cm^{-1}$) and additional cellular biomolecules. Higher frequency vibrations of CH bonds in lipids and proteins can be observed at higher wavenumbers $2700-3500\,cm^{-1}$ [9].

The main difficulties in analyzing the Raman spectra of histological sections are that the fixing substance — paraffin — has strong peaks in the spectral regions with high wave numbers. These peaks can be found on 892, 1065, 1135, 1174, 1298, 1421, 1443 and $1464\,cm^{-1}$, where they partially overlap with the Raman spectrum of the studied biological sample [10].

The contribution of paraffin to the Raman spectrum can be excluded either by chemical deparaffinization of the sample, or by computer processing of the spectrum with subtraction of the main peaks of paraffin from the measured spectrum [11]. In [12] it was shown that chemical dewaxing, as well as the fixation process itself, has a noticeable effect on the lipid content in samples, and therefore it should be used with caution when analyzing data based on changes in lipids. Digital processing of the spectra allows avoiding the specified molecular modification of the sample, but may limit the number of areas for confident interpretation.

It should be noted that many problems associated with chemical fixation and leaching of light elements could be avoided by using fast-freeze cryofixation [13]. Unfortunately, the complete chain of cryogenic processes „sample preparation — storage — measurement“ was not possible in our study.

Thus, the problem of a comprehensive study of biological samples using X-ray microscopy, fluorescence microanalysis and Raman spectroscopy is solved in this paper, for the first time, to determine the possible relationship between the accumulation of bound (non-osmotic) sodium and the distribution features of the main organic compounds, components of the structure of the intercellular space. As mentioned above, this study is also aimed at confirming or refuting the modern hypothesis [2] about the formed chemical bonds of sodium cations with glycosaminoglycan molecules in the analysis of the effect of salt intake on cardiac muscle dysfunction.

1. Preparation of samples

Fifteen male Wistar rats aged 15 to 16 weeks were divided into two groups with the same body weight, 297.4 ± 68.4 g (normal salt intake group) and 252.0 ± 67.4 g (excessive salt intake group). Starting from the third week, the rats were given different diets: the high-salt group received about 2 mEq of sodium in food per 200 g of body weight, the low-salt group — respectively about 0.2 mEq. After 8 weeks, muscle tissue samples from animals were removed and preserved in formalin.

3-micron thick sections of myocardial tissue and thigh muscles with fixation in paraffin were made in accordance with the standard histological procedure. Sections for histological analysis were stained and placed on slides. For X-ray microscopy, the corresponding sections were not stained and fixed on a thin ULTRALENE film with a thickness of $4\,\mu m$, and to obtain Raman spectra, the unstained sections were placed on a slide with an aluminum coating produced by magnetron sputtering.

2. Methods

X-ray studies of the distribution of inorganic materials (Na, Si, Ca, etc.) were carried out at two ELETTRA synchrotron workstations (Trieste, Italy): IAEA-XRF X-ray fluorescence microanalysis and TwinMic scanning X-ray microscope stations. The IAEA-XRF station uses the radiation of the electron beam in a bending magnet. For our studies, the photon energy of the exciting beam was 3.5 keV, the size of the X-ray beam on the sample at an angle of incidence of 45° was about $100\times200\,\mu m$ at a flux of $> 10^9$ photons/s. X-ray fluorescence spectra were taken using a silicon drift detector (SDD) Bruker Nano GmbH, XFlash 5030 with a spectral resolution of 131 eV on the Mn *K*-line. The experimental layout allowed two-dimensional scanning of the sample to obtain a distribution map of chemical elements, starting from sodium [14].

The X-ray fluorescence microscopy station TwinMic [15] was used to obtain a map of the distribution of lighter elements from carbon to magnesium with high spatial resolution $\sim 1\,\mu m$. The microscope operated in scanning mode with the energy of the incident X-ray beam 1.472 keV. Simultaneously with the acquisition of absorption and phase-contrast X-ray images, the local spectrum of X-ray fluorescence was measured using seven SDD PNsensor detectors optimized for the soft X-ray range. The recording time of X-ray fluorescence spectra in one pixel of the image was 5–10 s during the scanning of the sample area. The PyMCA program and original Python scripts were used for quantitative processing of the spectra.

Raman spectra were measured using a Renishaw In Via Raman Microscope spectrometer (Renishaw, UK) equipped with a diode laser with a wavelength of 785 nm. A confocal microscope is integrated into the design of the device, which makes it possible to obtain images of the studied samples both in white light and at Raman scattering frequencies for mapping the distribution of compounds with a spatial resolution of up to $2\,\mu m$. NPlan 50/0.50 lens with an operating distance of 8 mm (Leica, Germany) was used in our experiments to obtain spectra and microscopic images. The measurement time was 100 s, spectral resolution — $1\,cm^{-1}$. The power in the focus was decreased down to decreased 0.1–0.5% of 45 mW of the initial laser beam power to prevent melting and burning of the paraffin-containing material. The measured Raman spectra were analyzed using Renishaw software (Renishaw FixtureBuilderx64) and Origin 8.5

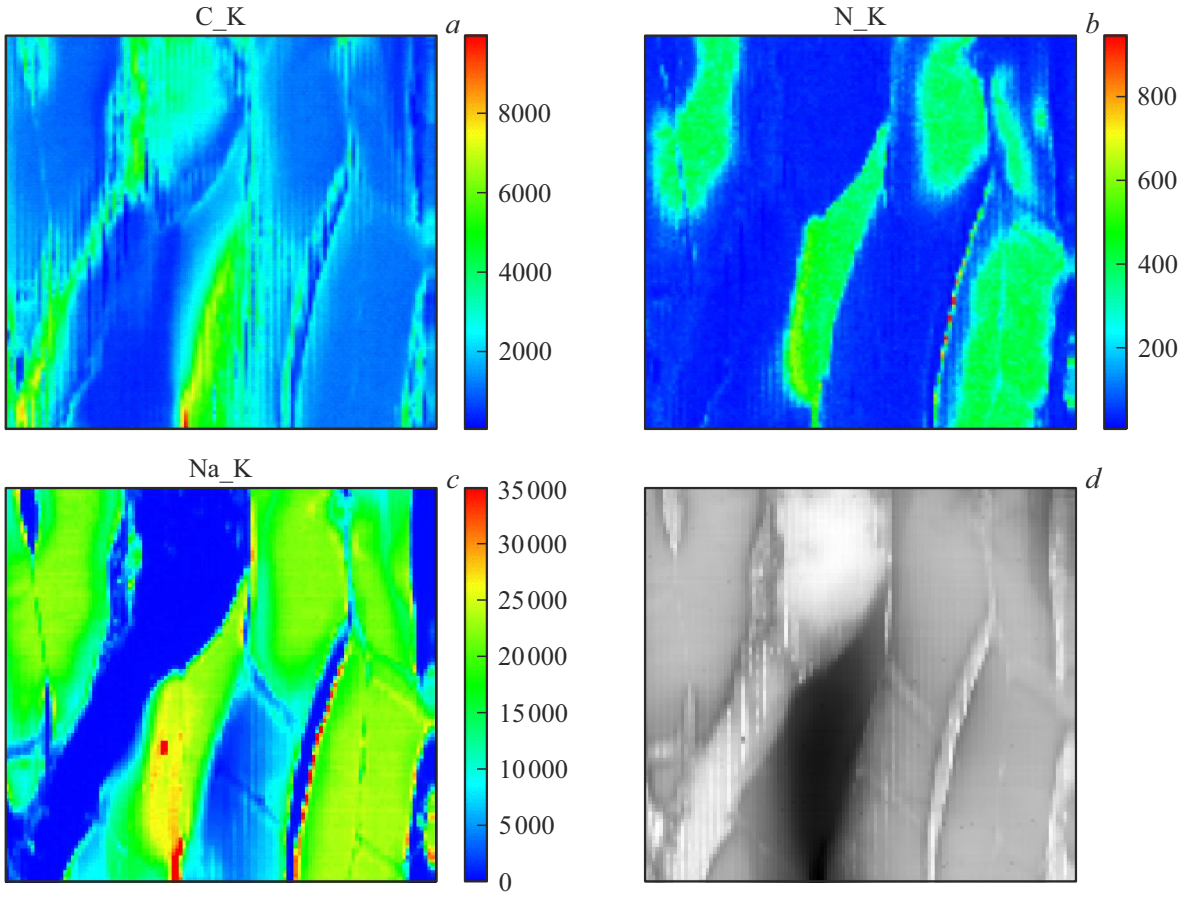

Figure 1. Distribution maps of carbon (a), nitrogen (b) sodium (c), and corresponding X-ray absorption image (d) of a cross-striated muscle section. Scan size $300\times275\,\mu$m.

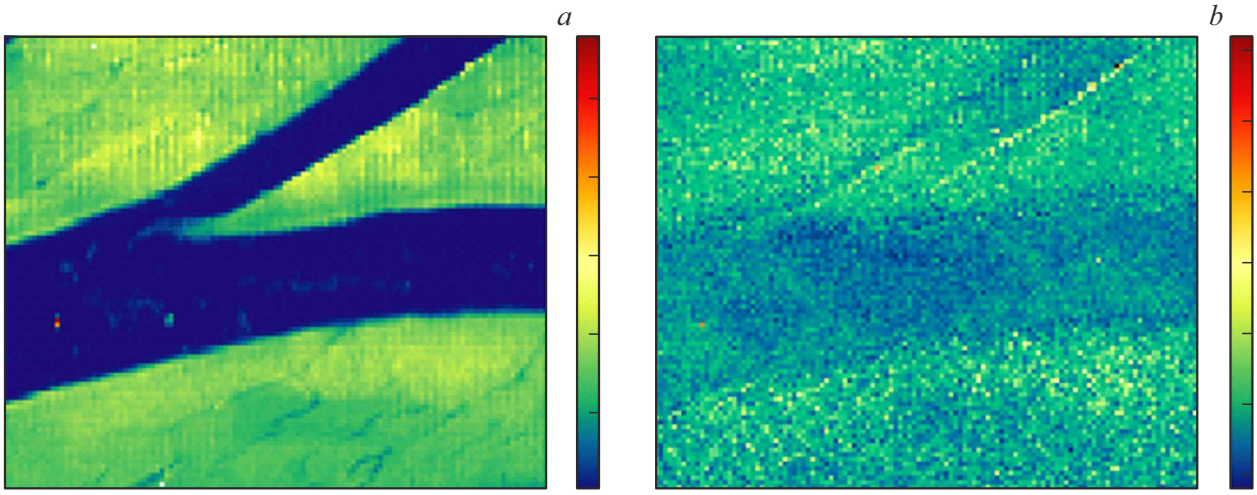

Figure 2. Distribution of sodium (a) and iron (b) in cells and the intercellular space (interstitial) of the striated thigh muscle of the rat. The dark blue color (in the online version) indicates the intercellular space. Scan size $200\times200\,\mu$m.

3. Results

The data obtained at synchrotron workstations on the intensity of X-ray fluorescence when scanning histological sections were used to map the distribution of various chemical elements (Fig. 1).

Fig. 2 shows a map of the distribution of sodium and iron in the cells and intercellular space (interstitial) of the striated

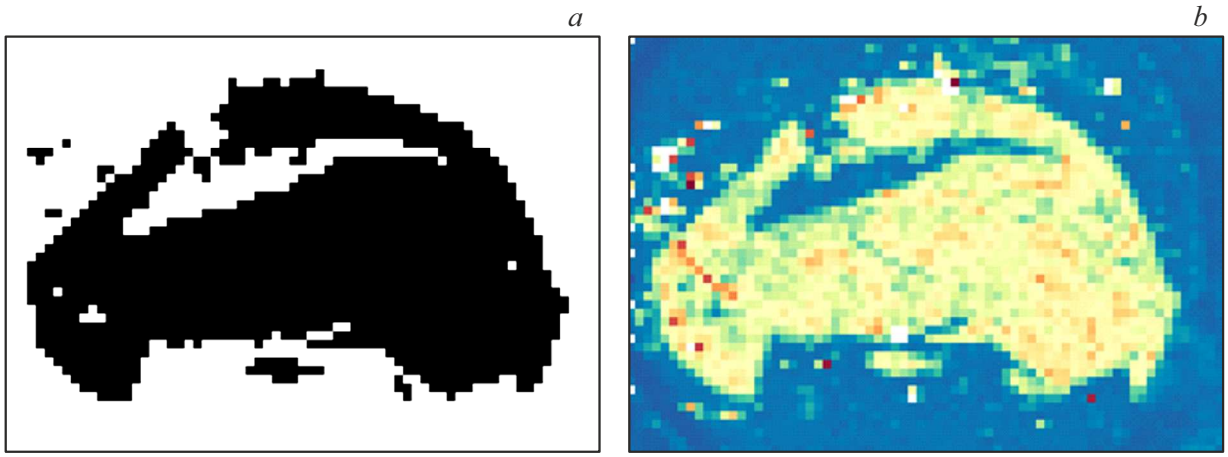

Figure 3. Cluster segmentation of the image to determine the boundaries of the tissue slice (*a*) using a map of the distribution of sulfur (*b*).

thigh muscle of a rat. In Fig. 2, *a*, the peak of the point concentration of sodium in the left part of the intercellular space is clearly visible, while the presence of iron atoms in the intercellular space indicates that in this case an image of the microstructure element of the tissue — interstitial, and not, for example, cracks filled with paraffin (fig. 2, *b*).

An algorithm of agglomerative clustering using *K*-lines of sulfur and phosphorus was applied for segmentation of element distribution maps. At the very beginning of the algorithm, each pixel was defined as a separate cluster. Then, at each step, the algorithm connected clusters with similar values into one whole. The procedure ended when there were only two clusters corresponding to the empty part of the substrate film and the area of the slice sample under study (Fig. 3).

Fig. 4 demonstrates the results obtained by measuring the Raman spectra of the histological section in the cells and at the border of the intercellular space of the myocardium, at several points marked in the image. In corresponding characteristic spectra, a set of peaks characteristic of biological samples (cells, tissues, etc.) is observed. [9], which is markedly different from the observed spectrum of paraffin present in the sample. A wide band in the region of 1600–1700 cm^{-1} is a well-known band/peak of Amide I and is attributed primarily to vibrations in peptide bonds (CN) in proteins and proteins, as well as C=C-groups in unsaturated lipids and in carbohydrates. The Amide I band is a superposition of bands characteristic of proteins with different secondary structures, so its detailed analysis allows determining the condition of the protein and the impact of its environment on its properties [16]. It can be assumed that the observed shift of the maximum of the peak of Amide I for the spectra measured in cells and at the boundary of the intercellular space is associated with the sensitivity of Amide I to the immediate environment of the protein and the effect on it of the heterogeneous distribution of chemical elements in tissues.

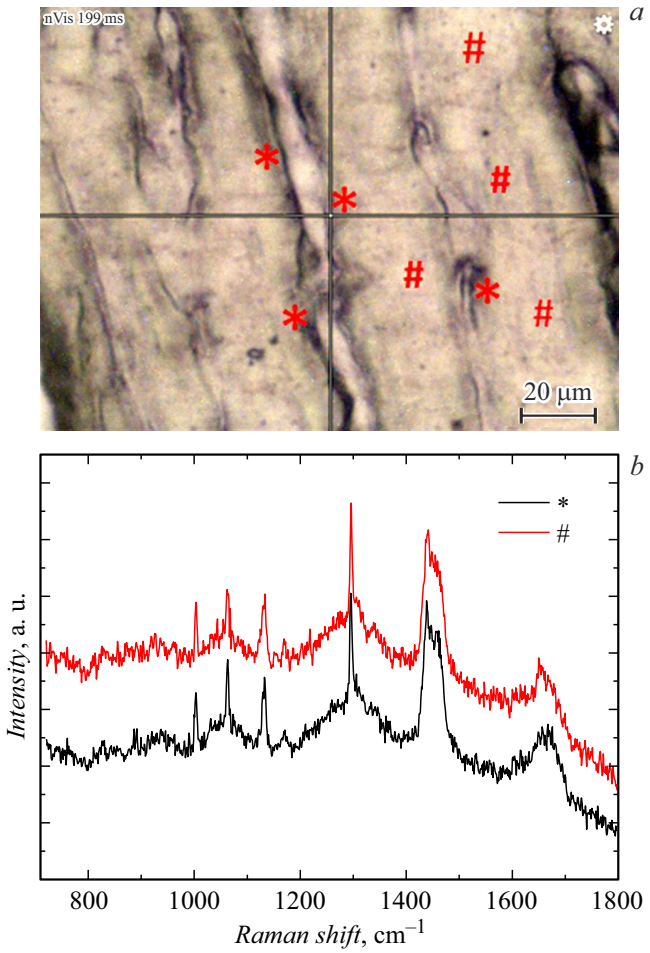

Figure 4. An image of an unstained histological slice with the designated measurement points of the Raman spectra (*a*) and averaged spectra measured at these points (*b*).

An intense band with a maximum of about 1445 cm^{-1} is produced as a result of vibrations in CH groups in

lipids, as well as vibrations in CH_2- and CH_3-groups in lipids and proteins. Amide III band also belonging to the protein is observed in $1200-1300\,cm^{-1}$. Vibrations in the groups of CH- and CH_2 in lipids are visible in the range of $1290-1340\,cm^{-1}$; vibrations in C−O- and C−O−H-groups of carbohydrates are visible in the range of $1020-1140\,cm^{-1}$. The observed vibrations in the range of $700-1300\,cm^{-1}$ are attributed to amino acids. In particular, the narrow band in $1002-1004\,cm^{-1}$ is an oscillation of the aromatic ring of the phenylalanine molecule. Note that its intensity and maximum position are not sensitive to conformational changes in protein and are often used as a reference point in the analysis and calibration of the Raman spectra of both proteins and biological systems as a whole [17].

Narrow peaks at 1065, 1135 and $1298\,cm^{-1}$, as well as peaks contributing to the intensity of the Raman signal in the region of $1440-1460\,cm^{-1}$, belong to paraffin [10].

Conclusion

The conducted studies in the X-ray and infrared spectral ranges confirmed the possibility of determining traces of chemical elements and compounds left after the procedure of histological treatment and chemical fixation with paraffin. The high spatial resolution of both spectroscopic methods makes it possible to make maps of the distribution of various biochemical substances and monitor their features, in particular during the differential study of muscle tissue samples taken from laboratory animals divided into groups. Thus, with a comprehensive study of the same area of a tissue sample, complementary data on the correlation of the location of inorganic elements and bioorganic materials can be obtained, which allows identifying the biochemical mechanisms of binding of light cations.

X-ray absorption images were acquired at the cellular level of sections of various muscle tissues using synchrotron radiation and their chemical composition was analyzed to solve the problem of searching and identifying sodium deposits inside the extracellular space.

The local Raman spectra were measured at various points of the histological section: in the cells of the striated muscle and at the border of the intercellular space. A set of peaks characteristic of biological tissues is marked in the spectra, while the maximum peak of Amide I in the spectra measured at the boundary of the intercellular space is shifted relative to Amide I in the cell spectra. It is assumed that the accumulation of sodium in the intercellular space can affect Amide I due to its sensitivity to the immediate environment of the protein.

Thus, the basis of new methods of complex studies of standard histological sections based on a combination of X-ray and infrared analytical microscopy for the search and identification of both inorganic elements and organic compounds was developed.

Further development of a combination of several spectromicroscopic methods of biochemical analysis will significantly expand the scope of effective application of each method and improve their informative value. In addition, the development of methods for working with standard histological sections will significantly speed up and simplify the preparation of samples and will allow collecting more data for statistical analysis.

Acknowledgments

The studies as part of project №20195340 at the ELETTRA synchrotron were financially supported by the IAEA under the Agreement between the IAEA and the ELETTRA-Synchrotron-Trieste. The authors are grateful to A. Gianoncelli and S. Pollastri for their help in this work.

Conflict of interest

The authors declare that they have no conflict of interest.

References

[1] D. Mozaffarian, S. Fahimi, G.M. Singh, R. Micha, S. Khatibzadeh, R.E. Engell, S. Lim, G. Danaei, M. Ezzati, J. Powles. NEJM, **371**, 624 (2014). DOI: 10.1056/NEJMoa1304127

[2] J. Titze, H. Krause, H. Hecht, P. Dietsch, J. Rittweger, R. Lang, K.A. Kirsch, K.F. Hilgers. Am. J. Physiol. Renal Physiol., **283**, F134 (2002). DOI: 10.1152/ajprenal.00323.2001

[3] I. Artyukov, G. Arutyunov, M. Bobrov, I. Bukreeva, A. Cedola, D. Dragunov, R. Feshchenko, M. Fratini, V. Mitrokhin, A. Sokolova, A. Vinogradov, A. Gianoncelli. Sci. Rep., **11** (1), 22025 (2021). DOI: 10.1038/s41598-021-01443-8

[4] T. Paunesku, S. Vogt, J. Maser, B. Lai, G. Woloschak, J. Cell. Biochem., **99** (6), 1489 (2006). DOI : 10.1002/jcb.21047

[5] C. Poitry-Yamate, A. Gianoncelli, B. Kaulich, G. Kourousias, A.W. Magill, M. Lepore, V. Gajdosik, R. Gruetter. J. Neurosci. Res., **91** (8), 1050 (2013). DOI: 10.1002/jnr.23171

[6] L. Merolle, M. Ragazzi, A. Gianoncelli, M. Altissimo, A. Ciarrocchi, D. Bedolla, C. Marraccini, R. Baricchi, T. Pertinhez. JINST, **13** (5), C05018 (2018). DOI: 0.1088/1748-0221/13/05/C05018

[7] K. Ikemoto, K. Hashimoto, Y. Harada, Y. Kumamoto, M. Hayakawa, K. Mochizuki, K. Matsuo, K. Yashiro, H. Yaku, T. Takamatsu. AHC, **54** (2), 65 (2021). DOI: 10.1267/ahc.21-00016

[8] H.J. Butler, L. Ashton, B. Bird, G. Cinque, K. Curtis, J. Dorney, K. Esmonde-White, N.J. Fullwood, B. Gardner, P.L. Martin-Hirsch. Nat. Protoc., **11** (4), 664 (2016). DOI: 10.1038/nprot.2016.036

[9] Z. Movasaghi, S. Rehman, I.U. Rehman. Appl. Spectrosc. Rev., **42** (5), 493, (2007). DOI: 10.1080/05704920701551530

[10] A. Tfayli, C. Gobinet, V. Vrabie, R. Huez, M. Manfait, O. Piot. Appl. Spectrosc., **63** (5), 564 (2009). DOI: 10.1366/000370209788347048

[11] S.M. Ali, F. Bonnier, A. Tfayli, H. Lambkin, K. Flynn, V. McDonagh, C. Healy, T. Clive Lee, F.M. Lyng, H.J. Byrne. J. Biomed. Opt., **18** (6), 061202 (2013). DOI: 10.1117/1.JBO.18.6.061202
[12] M.M. Mariani, P. Lampen, J. Popp, B.R. Wood, V. Deckert. Analyst, **134** (6), 1154 (2009). DOI: 10.1039/b822408k
[13] L. Merolle, L. Pascolo, L. Zupin, P. Parisse, V. Bonanni, G. Gariani, S. Kenig, D.E. Bedolla, S. Crovella, G. Ricci. Molecules, **28** (4), 1992 (2023). DOI: 10.3390/molecules28041992
[14] A.G. Karydas, M. Czyzycki, J.J. Leani, A. Migliori, J. Osan, M. Bogovac, P. Wrobel, N. Vakula, R. Padilla-Alvarez, R.H. Menk. J. Synchrotron Radiat., **25** (1), 189 (2018). DOI: 10.1107/S1600577517016332
[15] A. Gianoncelli, G. Morrison, B. Kaulich, D. Bacescu, J. Kovac. Appl. Phys. Lett., **89** (25), 251117 (2006). DOI: 10.1063/1.2422908
[16] A. Barth, C. Zscherp. Q. Rev. Biophys., **35** (4), 369 (2002). DOI: 10.1017/S0033583502003815
[17] C. Krafft, T. Knetschke, R.H.W. Funk, R. Salzer, Anal. Chem., **78**, 4424 (2006). DOI: 10.1021/ac060205b

Translated by A.Akhtyamov